

Preparation of Spherical Nanocellulose from Waste Tobacco Stem

Fanghan Luo,^{b,1} Xueju Xu,^{b,1} Yongze Jiang,^b Jinqiu Qi,^b Jian Zhou,^{a,*} Yaxi Liu,^{c,*} and Shaobo Zhang^{b,*}

Tobacco stems constitute a large amount of waste biomass generated during tobacco production, and their recycling is of great significance to the environment and the conservation of resources. In this study, an efficient, inexpensive, and less toxic strategy is reported for recycling waste tobacco stem, wherein the spherical tobacco stem nanocellulose (STsN) with a size of 10 to 100 nm was prepared from waste stems using a NaOH/urea/thiourea aqueous system. The morphology of STsN was characterized using scanning electron microscopy. The crystal structure of STsN was determined using X-ray diffractometry. The nanocellulose exhibited the crystal structure of cellulose II. Fourier-transform infrared spectra of the STsN indicated that STsN retained the typical chemical structure of cellulose. The thermal properties of STsN were investigated by thermogravimetry. It is concluded that the STsN had better thermal stability than cellulose. The product has potential for practical application with high thermal stability requirements, such as transistors and batteries.

DOI: 10.15376/biores.19.2.3826-3836

Keywords: Spherical nanocellulose; Waste tobacco stem; Cellulose II

Contact information: a: China Tobacco Sichuan Industrial Co., Ltd., Harmful Components and Tar Reduction in Cigarette Key Laboratory of Sichuan Province, Chengdu, China; b: Wood Industry and Furniture Engineering Key Laboratory of Sichuan Provincial Department of Education, College of Forestry, Sichuan Agricultural University, Chengdu, China; c: State Key Laboratory of Crop Gene Exploration and Utilization in Southwest China, Sichuan Agricultural University, Chengdu, China; ¹ These authors contributed equally to this work.

* Corresponding authors: zhoujian8860@163.com; liuyaxi@sicau.edu.cn; shaobo_z@sicau.edu.cn

INTRODUCTION

During the production and manufacture of finished cigarette products, large amounts of tobacco waste are inevitably generated, as well as waste is produced in the re-roasting process, such as broken tobacco dust and long stems (Banožić *et al.* 2020; Saleem *et al.* 2022). Statistics have shown that tobacco cultivation and cigarette manufacturing have generated up to 200 million tons of tobacco waste annually in recent years (Hoe *et al.* 2022). Tobacco biomass mainly contains tobacco stem, tobacco shreds, and tobacco leaf fragments (Patskan and Reininghaus 2003; Jian *et al.* 2010). Among them, tobacco stems have a rich fiber content (up to 23%), which are higher than that of the leaf lamina. However, as a by-product of the tobacco production, more than 60% of tobacco stems are disposed of as garbage worldwide after the tobacco leaves are harvested (Chen *et al.* 2017; Yan *et al.* 2018; Zhang *et al.* 2019a), which leads to a considerable waste of natural plant resources and causes serious environmental pollution (Fan *et al.* 2022).

Nanocellulose has the potential for diverse applications because of its several exceptional properties, such as nanoscale effects, biodegradability, biocompatibility, high strength, and strong surface activity (Zhang *et al.* 2019b). Several studies have been published on the preparation of nanocellulose from various raw materials such as wood (Sirviö *et al.* 2020), cotton (Morais *et al.* 2013; Chen *et al.* 2014), bamboo (Razalli *et al.* 2017;), straw (Kaushik and Singh 2011), agricultural waste (Cherian *et al.* 2011; Visakh *et al.* 2012; Faradilla *et al.* 2016), and recycled pulp (Sehaqui *et al.* 2016). Because the natural form of cellulose is fibrous, most studies have prepared rod-shaped and fibrous nanocellulose. However, compared to common fibrous and rod-shaped nanocellulose, spherical nanocellulose has additional properties because of its spherical morphology. For example, spherical nanocellulose of the same diameter typically has a larger specific surface area and a higher surface-functional-group density (Yu *et al.* 2017; Hafemann *et al.* 2019).

Zhang *et al.* (2007) prepared spherical nanocellulose with sizes ranging from 60 to over 570 nm by pretreating cellulose with NaOH and DMSO, followed by treatment with mixed acids for 8 h. In 2018, the Chauhan team used the same method to prepare spherical nanocellulose, which was functionally modified to be used as naked-eye sensor, rapid adsorbent and antimicrobial agent. (Ram *et al.* 2018; Ram and Chauhan 2018). Yan *et al.* (2015) prepared spherical nanocellulose with particle size of 19 to 29 nm by one-step HCOOH/HCl hydrolysis of lyocell fibers with cellulose II crystal structure. This makes these nanospheres effective templates for synthesizing nanohybrids and high-nanocomposite reinforcements (Yan *et al.* 2015). Ahmed-Haras *et al.* (2020) used a rapid single-step heterogeneous hydrolysis technique to prepare highly monodispersed spherical nanocrystalline cellulose (SNCC) with an average diameter of 36 nm. Increased resistance to thermal degradation was observed for SNCC compared to microcrystalline cellulose (MCC), producing a final residue with thrice higher resistance and a maximum decomposition temperature of 391 °C. As a result, the nanocellulosic materials prepared using the heterogeneous acid-catalyzed method exhibited improved crystallinity and morphological and thermal properties (Ahmed-Haras *et al.* 2020). Zhang *et al.* (2021) prepared spherical bamboo nanocellulose (SBN) with an average particle size of 61 nm from bamboo powder using a NaOH/urea/thiourea aqueous system. The SBN exhibited a cellulose II crystal structure. Creative SBN/Fe₃O₄ composite films were prepared. The results revealed that the dispersion of Fe₃O₄ nanoparticles in the SBN/Fe₃O₄ composite films was much better than that in the nanofibrillated cellulose (NFC)/Fe₃O₄ composite films, and the highest transmittance of the films was higher than that of the NFC/Fe₃O₄ composite films with the same amount of Fe₃O₄ (Zhang *et al.* 2021).

In this study, industrial waste was utilized to produce spherical nanocellulose. A practical and effective pretreatment method using sodium chlorite/glacial acetic acid to obtain bleached cellulose from waste tobacco stems as raw materials was proposed. The authors subsequently developed an efficient, inexpensive, and less toxic strategy to prepare spherical tobacco stem nanocellulose (STsN) *via* NaOH/thiourea/urea aqueous system. Finally, the STsN using Fourier-transform infrared (FTIR) spectroscopy, X-Ray Diffraction (XRD), scanning electron microscopy (SEM), transmission electron microscope (TEM), and thermo gravimetric (TG) was examined.

EXPERIMENTAL

Materials

Waste tobacco stems were collected as raw materials. NaOH, thiourea, and urea were purchased from Sinopharm Chemical Reagent Co., Ltd. (Shanghai, China). Sodium chlorite, glacial acetic acid, and anhydrous ethanol were purchased from the China National Pharmaceutical Group Chemical Reagent Co., Ltd. (Shanghai, China). All the chemicals were analytically unmixed and used without further purification.

Pretreatment

The raw material was crushed into a powder and cleaned with hot water at 80 °C for 60 min to remove water-soluble impurities. The bleaching treatment was conducted by combining 6 mL icy acetic acid and 9 g of sodium chlorite in 350 mL of water for 1 h at 75 °C. This process was repeated 10 times until colored substances were removed. The samples were then cleaned with deionized water until the filtrate was neutral. Eventually, the bleached tobacco stem cellulose was successfully prepared.

Preparation of STsN

A 200 mL aqueous solution of 8 wt% NaOH, 8 wt% urea, and 6.5 wt% thiourea was pre-cooled to −10 °C. Subsequently, 2 g of bleached tobacco stem cellulose was dispersed into the solution, which was then vigorously stirred for 50 min. The insoluble fractions were separated by centrifugation at 11000 rpm for 20 min to obtain a translucent solution. Subsequently, 2000 mL deionized water was added dropwise to the transparent solution for 30 min and simultaneously slowly stirred until 100% of the cellulose was regenerated to obtain a thick white suspension. Deionized water was used to rinse the suspension several times until the pH reached 7. After cleaning, the suspension was sonicated at 600 W for 60 min, and the impurities were removed by centrifugation at 11000 rpm for 20 min to obtain the STsN suspension. The STsN percentage yield was calculated from Eq. 1, using the pre-recorded values of the bleached tobacco stem cellulose mass initially dispersed into the solution (W_m) and the prepared STsN mass (W_n):

$$\text{Percent Yield} = \frac{W_n}{W_m} \times 100 \quad (1)$$

Methods

X-ray diffraction (XRD)

The XRD patterns were obtained using a Japan-Rigaku-SmartLab 9-kW diffractometer. The specimens were scanned stepwise over the operational range of the scattering angle, between 5° and 40°. The scanning speed was 5°/min.

Degree of polymerization (DP)

The average degree of polymerization was determined using Eq. 2 (Xiong *et al.* 2012),

$$DP^{0.905} = 0.75 [\eta] \quad (2)$$

where $[\eta]$ is the intrinsic viscosity ($\text{cm}^3 \text{g}^{-1}$) of copper-ethylenediamine solution determined using ASTM D1795-13 (2013) (Pintiaux *et al.* 2019; Rosson and Byrne 2022). In brief, the dried sample was dissolved in a copper-ethylenediamine solution at 25 °C. The

term $[\eta]c$ (where c is the cellulose concentration) of the solution was calculated using the efflux time of the sample solution, obtained using a Cannon-Fenske capillary viscometer, according to the ASTM D1795-13 (2013) standard. Subsequently, $[\eta]$ was obtained. All experiments were performed in triplicate.

Fourier transform infrared spectroscopy (FTIR)

The FTIR data were collected using a Thermo Fisher Nicolet iS5 spectrometer (Thermo Fisher, Waltham, MA, USA). The samples were examined in transmission mode in the spectral range of 400 to 4000 cm^{-1} .

Scanning electron microscopy (SEM) analysis

The SEM images of the bleached tobacco stem cellulose and STsN were captured using a Zeiss Gemini 300 microscope (Carl Zeiss, Jena, Germany). The STsN suspension was dried to obtain the STsN specimens. All samples were sputter-coated with platinum (Oxford Quorum SC7620, Quorum Technologies, East Sussex, UK).

Transmission electron microscope (TEM) analysis

The TEM images of STsN was performed using a Talos F200s microscope (Thermo Scientific, Waltham, USA). The STsN suspension was dried by depositing a droplet onto a film on a copper grid and subsequently observed using a 200 kV accelerating voltage.

Thermo gravimetric (TG) analysis

The thermo gravimetric (TG) analysis of the samples was measured using a TA SDT 650 (China) thermal analyzer under a nitrogen atmosphere, data were recorded from 30 to 800 $^{\circ}\text{C}$ with a heating rate of 10 $^{\circ}\text{C}$ per min.

RESULTS AND DISCUSSION

Morphological Characterization

As can be seen from a photograph of the raw materials in Fig. 1a, the crushed tobacco stems appeared as a dark-brown powder. After the pretreatment, the bleached tobacco stem cellulose appeared as a white powder (Fig. 1b). The DP of the bleached tobacco stem cellulose was 299. The SEM images of the bleached tobacco stem cellulose are presented in Fig. 1c. The material exhibited a lump structure, whose diameter was around 120 μm and mean length was approximately 285 μm . Figure 1d shows the STsN solution as a well dispersed suspension state, which is the typical morphology of nanoparticle suspensions. The micromorphology of STsN was characterized using SEM and TEM (Figs. 1e-1h). The images showed that STsN exhibited a three-dimensional spherical shape with a particle size of 10 to 100 nm. Thus, according to the SEM and TEM analysis, the spherical tobacco stem nanocellulose with nanoscale particle size were successfully prepared using a NaOH/thiourea/urea aqueous system. In addition, the yield of STsN obtained by this preparation process was calculated as 55.9%.

Under low-temperature conditions, NaOH, urea, and thiourea are recognized to synergistically contribute to the dissolution process of cellulose (Jin *et al.* 2007). At low temperatures, the NaOH hydrate is more adept at disrupting the hydrogen bonds between cellulose chains (Zhang *et al.* 2010). Urea and thiourea hydrates can self-assemble on the surface of NaOH/cellulose complexes, forming relatively stable inclusion complexes,

thereby facilitating cellulose dissolution (Cai *et al.* 2008a). Complexes associated with cellulose chains, NaOH, urea, thiourea, and water clusters undergo bending into spherical shapes due to the disruption of intermolecular hydrogen bonds (Jiang *et al.* 2012). After cellulose dissolution, nanocellulose is regenerated by introducing deionized water into the cellulose solution. Upon water addition, the concentrations of sodium hydroxide, thiourea, and urea in the complexes decrease. Since water acts as a poor solvent for cellulose, cellulose chains aggregate and precipitate slightly, resulting in the formation of spherical nanocellulose (Cai *et al.* 2008b; Lou *et al.* 2015; Zhang *et al.* 2019b).

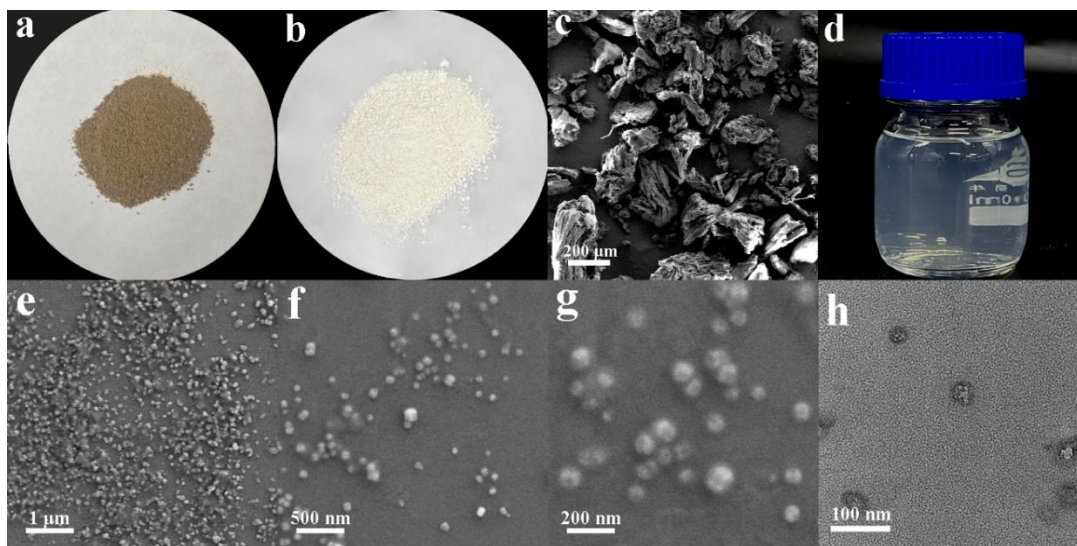


Fig. 1. Photographs of tobacco stem powder (a), bleached tobacco stem cellulose (b), and STsN suspension (d). SEM images of bleached tobacco stem cellulose (c) and increasing-magnification STsN (e-g). TEM image of STsN (h). The amount of solids of STsN was diluted by 50X.

Basic Structure Characterization of STsN

The XRD analysis of the STsN was performed to investigate the crystal structure of the samples (Fig. 2).

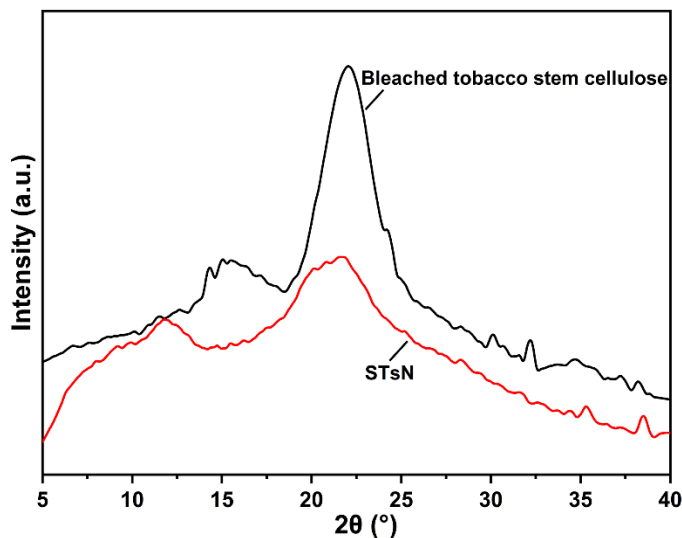


Fig. 2. XRD spectra of the bleached tobacco stem cellulose (the sample in the Fig.1c) and STsN

In the XRD spectrum of the bleached tobacco stem cellulose, the peaks at 15.0° , 16.7° , 22.2° , and 34.6° correspond to the Miller indices of (1–10), (110), (200), and (004), respectively, and reveal a typical cellulose I crystal structure (French 2014). The XRD spectrum of STsN exhibited three diffraction peaks, located at 11.9° , 20.4° , and 21.7° . The three main peaks in the XRD spectra of STsN had Miller indices of (1–10), (110), and (020). This is a typical feature of the crystal structure of cellulose II (French 2014), and is common in regenerated cellulose (Zhang *et al.* 2021, 2023).

Figure 3 shows the FTIR spectra of the bleached tobacco stem cellulose and STsN. The FTIR spectrum of the bleached tobacco stem cellulose showed typical peak levels of cellulose I. The peaks from 3700 to 3100 cm^{-1} were attributed to the fundamental modes of O–H, which are dependent on the carbohydrates and vibrations of the hydrogen-bonded hydroxyl groups (Alemdar and Sain 2008). The peaks at 2914 , 1632 , and 895 cm^{-1} are attributed to the C–H stretching vibration, the C–C stretching band, and the glycosidic stretchy bond, respectively (Coleman *et al.* 1988; Yang *et al.* 2007; Trache *et al.* 2014). The peaks at 1160 cm^{-1} and 1020 cm^{-1} are due to the C–O stretching of secondary hydroxyl and primary hydroxyl (Huang *et al.* 2017). These demonstrated that the bleached tobacco stem cellulose was successfully extracted from waste tobacco stems.

Although the FTIR spectrum of STsN is similar to those of the bleached tobacco stem cellulose, maintaining typical cellulose characteristic peaks, it exhibits significant differences. The strong peak at 1428 cm^{-1} assigned to CH_2 scissoring motion in cellulose became weakened and shifted to 1420 cm^{-1} in STsN. This indicates the structural change in the conformation of CH_2OH at C6 position from trans-gauche (*tg*) to gauche-trans (*gt*), which confirms the change of crystal structure from cellulose I to cellulose II (Ruan *et al.* 2004; Zhang *et al.* 2009). This is consistent with the results of the XRD analysis.

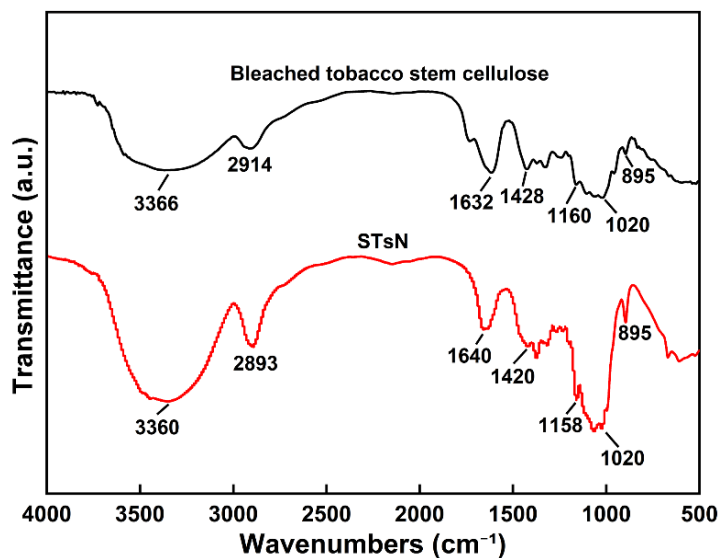


Fig. 3. FTIR spectra of the bleached tobacco stem cellulose and STsN

Thermal Properties of STsN

The TG analysis results of the bleached tobacco stem cellulose and STsN are shown in Fig. 4. The initial decomposition temperature (IDT) of the STsN was 257°C , which was higher than that of bleached tobacco stem cellulose (234°C). This revealed that the thermal stability of the STsN was better than that of bleached tobacco stem cellulose, which was caused by the cellulose II crystal structure of STsN. Due to the different orientation of the

cellulose chains and hydrogen bonding patterns in cellulose I and cellulose II, cellulose II is generally more thermally stable than cellulose I (Adsul *et al.* 2012).

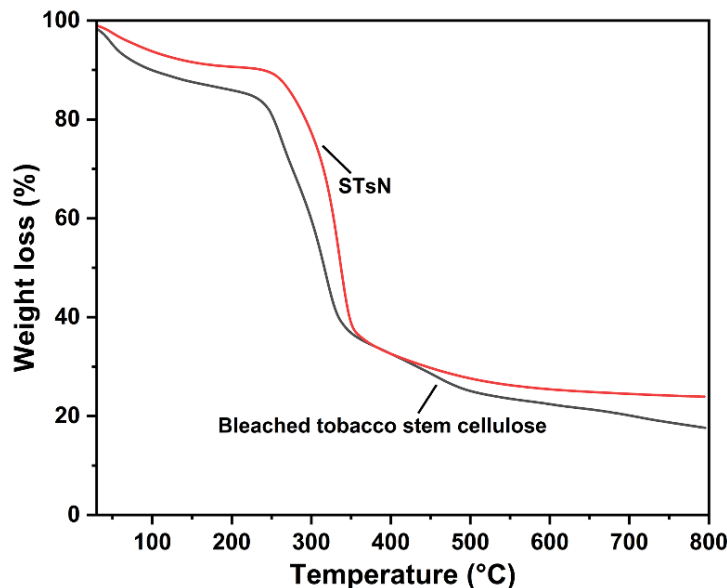


Fig. 4. The TG curves of the bleached tobacco stem cellulose and STsN

CONCLUSIONS

1. In this study, spherical tobacco stem nanoparticles (STsNs) were prepared from waste tobacco stems using a NaOH/thiourea/urea aqueous system. The morphology of the nanocellulose was investigated using scanning electron microscopy (SEM) and transmission electron microscopy (TEM). The images showed a clear three-dimensional spherical shape with a particle size of 10 to 100 nm.
2. Both X-ray diffraction (XRD) and Fourier transform infrared (FTIR) spectroscopy examined the basic crystal structure and chemical structure of STsN. Sharp diffraction peaks occurred at 11.9°, 20.4°, and 21.7°, all of which were consistent with a cellulose II crystal structure. The FTIR spectra of STsN were collected, which further confirmed the transformation of cellulose I to cellulose II during dissolution, and the STsN maintained the typical chemical structure of cellulose.
3. The thermogravimetric (TG) results showed that the IDT of the STsN was approximately 257 °C higher than that of bleached tobacco stem cellulose. This indicates that STsN exhibits better thermal stability and has potential for practical applications with high thermal stability requirements.

ACKNOWLEDGMENTS

This work was supported by the Opening Fund of Harmful Components and Tar Reduction in Cigarette Key Laboratory of Sichuan Province (jykf202201). Science and Technology Project of China Tobacco Sichuan Industrial Co., Ltd. (10202314BA510).

REFERENCES CITED

- Adsul, M., Soni, S. K., Bhargava, S. K., and Bansal, V. (2012). "Facile approach for the dispersion of regenerated cellulose in aqueous system in the form of nanoparticles," *Biomacromolecules* 13, 2890-2895. DOI: 10.1021/bm3009022
- Ahmed-Haras, M. R., Kao, N., and Ward, L. (2020). "Single-step heterogeneous catalysis production of highly monodisperse spherical nanocrystalline cellulose," *International Journal of Biological Macromolecules* 154, 246-255. DOI: 10.1016/j.ijbiomac.2020.02.298
- Alemdar, A., and Sain, M. (2008). "Isolation and characterization of nanofibers from agricultural residues - Wheat straw and soy hulls," *Bioresource Technology* 99(6), 1664-1671. DOI: 10.1016/j.biortech.2007.04.029
- ASTM D1795-13 (2013). "Standard test method for intrinsic viscosity of cellulose," ASTM International, West Conshohocken, PA, USA.
- Banožić, M., Babić, J., and Jokić, S. (2020). "Recent advances in extraction of bioactive compounds from tobacco industrial waste-a review," *Industrial Crops and Products* 144, article ID 112009. DOI: 10.1016/j.indcrop.2019.112009
- Cai, J., Kimura, S., Wada, M., Kuga, S., and Zhang, L. (2008a). "Cellulose aerogels from aqueous alkali hydroxide-urea solution," *Chemosuschem* 1(1-2), 668-674. DOI: 10.1002/cssc.200700039
- Cai, J., Zhang, L., Liu, S., Liu, Y., Xu, X., Chen, X., Chu, B., Guo, X., Xu, J., Cheng, H., Han, C. C., and Kuga, S. (2008b). "Dynamic self-assembly induced rapid dissolution of cellulose at low temperatures," *Macromolecules* 41(23), 9345-9351. DOI: 10.1021/ma801110g
- Chen, R., Li, L., Liu, Z., Lu, M., Wang, C., Li, H., Ma, W., and Wang, S. (2017). "Preparation and characterization of activated carbons from tobacco stem by chemical activation," *Journal of the Air and Waste Management Association* 67(6), 713-724. DOI: 10.1080/10962247.2017.1280560
- Chen, W., Abe, K., Uetani, K., Yu, H., Liu, Y., and Yano, H. (2014). "Individual cotton cellulose nanofibers: Pretreatment and fibrillation technique," *Cellulose* 21(3), 1517-1528. DOI: 10.1007/s10570-014-0172-z
- Cherian, B. M., Leão, A. L., de Souza, S. F., Costa, L. M. M., de Olyveira, G. M., Kottaisamy, M., Nagarajan, E. R., and Thomas, S. (2011). "Cellulose nanocomposites with nanofibres isolated from pineapple leaf fibers for medical applications," *Carbohydrate Polymers* 86(4), 1790-1798. DOI: 10.1016/j.carbpol.2011.07.009
- Coleman, M. M., Skrovanek, D. J., Hu, J., and Painter, P. C. (1988). "Hydrogen bonding in polymer blends. 1. FTIR studies of urethane-ether blends," *Macromolecules* 21(1), 59-65. DOI: 10.1021/ma00179a014
- Fan, X., Zi, W., Ao, J., Li, B., Qiao, J., Wang, Y., and Nong, Y. (2022). "Analysis and application evaluation of the flavour-precursor and volatile-aroma-component differences between waste tobacco stems," *Heliyon* 8(9), article ID e10658. DOI: 10.1016/j.heliyon.2022.e10658
- Faradilla, R. H. F., Lee, G., Rawal, A., Hutomo, T., Stenzel, M. H., and Arcot, J. (2016). "Nanocellulose characteristics from the inner and outer layer of banana pseudo-stem prepared by TEMPO-mediated oxidation," *Cellulose* 23(5), 3023-3037. DOI: 10.1007/s10570-016-1025-8
- French, A. D. (2014). "Idealized powder diffraction patterns for cellulose polymorphs," *Cellulose* 21(2), 885-896. DOI: 10.1007/s10570-013-0030-4

- Hafemann, E., Battisti, R., Marangoni, C., and Machado, R. A. F. (2019). "Valorization of royal palm tree agroindustrial waste by isolating cellulose nanocrystals," *Carbohydrate Polymers* 218, 188-198. DOI: 10.1016/j.carbpol.2019.04.086
- Hoe, C., Cohen, J. E., Yang, T., Peng, S., and Zhang, W. (2022). "Association of cigarette production and tobacco retailer density on secondhand smoke exposure in urban China," *Tobacco Control* 31(2), 118-125. DOI: 10.1136/tobaccocontrol-2021-056655
- Huang, J., Zhang, S., Zhang, F., Guo, Z., Jin, L., Pan, Y., Wang, Y., and Guo, T. (2017). "Enhancement of lignocellulose-carbon nanotubes composites by lignocellulose grafting," *Carbohydrate Polymers* 160, 115-122. DOI: 10.1016/j.carbpol.2016.12.053
- Jian, R. X., Feng, J. W., and Kai, L. (2010). "Sensory quality of tea recycled sheet and its use in cigarette," *Acta Agriculturae Jiangxi* 22(12), 61-62.
- Jiang, Z., Lu, A., Zhou, J., and Zhang, L. (2012). "Interaction between -OH groups of methylcellulose and solvent in NaOH/urea aqueous system at low temperature," *Cellulose* 19, 671-678. DOI: 10.1007/s10570-012-9669-5
- Jin, H., Zha, C, and Gu, L. (2007). "Direct dissolution of cellulose in NaOH/thiourea/urea aqueous solution," *Carbohydrate Research* 342(6), 851-858. DOI: 10.1016/j.carres.2006.12.023
- Kaushik, A., and Singh, M. (2011). "Isolation and characterization of cellulose nanofibrils from wheat straw using steam explosion coupled with high shear homogenization," *Carbohydrate Research* 346(1), 76-85. DOI: 10.1016/j.carres.2010.10.020
- Lou, H., Zhu, D., Yuan, L., Lin, H., Lin, X., and Qiu, X. (2015). "Fabrication and properties of low crystallinity nanofibrillar cellulose and a nanofibrillar cellulose-graphene oxide composite," *RSC Advances* 5(83), 67568-67573. DOI: 10.1039/C5RA13181B
- Morais, J. P. S., Rosa, M. de F., de Souza Filho, M. de sá M., Nascimento, L. D., do Nascimento, D. M., and Cassales, A. R. (2013). "Extraction and characterization of nanocellulose structures from raw cotton linter," *Carbohydrate Polymers* 91(1), 229-235. DOI: 10.1016/j.carbpol.2012.08.010
- Patskan, G., and Reininghaus, W. (2003). "Toxicological evaluation of an electrically heated cigarette. Part 1: Overview of technical concepts and summary of findings," *Journal of Applied Toxicology* 23(5), 323-328. DOI: 10.1002/jat.923
- Pintiaux, T., Heuls, M., Vandenbossche, V., Murphy, T., Wuhrer, R., Castignolles, P., Gaborieau, M., and Rouilly, A. (2019). "Cellulose consolidation under high-pressure and high-temperature uniaxial compression," *Cellulose* 26(5), 2941-2954. DOI: 10.1007/s10570-019-02273-8
- Ram, B., and Chauhan, G. S. (2018). "New spherical nanocellulose and thiol-based adsorbent for rapid and selective removal of mercuric ions," *Chemical Engineering Journal* 331, 587-596. DOI: 10.1016/j.cej.2017.08.128
- Ram, B., Chauhan, G. S., Mehta, A., Gupta, R., and Chauhan, K. (2018). "Spherical nanocellulose-based highly efficient and rapid multifunctional naked-eye Cr(VI) ion chemosensor and adsorbent with mild antimicrobial properties," *Chemical Engineering Journal* 349, 146-155. DOI: 10.1016/j.cej.2018.05.085
- Razalli, R. L., Abdi, M. M., Tahir, P. M., Moradbak, A., Sulaiman, Y., and Heng, L. Y. (2017). "Polyaniline-modified nanocellulose prepared from Semantan bamboo by chemical polymerization: Preparation and characterization," *RSC Advances* 7(41), 25191-25198. DOI: 10.1039/C7RA03379F

- Rosson, L., and Byrne, N. (2022). "Bicomponent regenerated cellulose fibres: Retaining the colour from waste cotton textiles," *Cellulose* 29(7), 4255-4267. DOI: 10.1007/s10570-022-04530-9
- Ruan, D., Zhang, L., Mao, Y., Zeng, M., Li, X. (2004). "Microporous membranes prepared from cellulose in NaOH/thiourea aqueous solution," *Journal of Membrane Science* 241(2), 265-274. DOI: 10.1016/j.memsci.2004.05.019
- Saleem, A., Hussain, A., Chaudhary, A., Ahmad, Q. A., Iqtedar, M., Javid, A., and Akram, A. M. (2022). "Acid hydrolysis optimization of pomegranate peels waste using response surface methodology for ethanol production," *Biomass Conversion and Biorefinery* 12(5), 1513-1524. DOI: 10.1007/s13399-020-01117-x
- Sehaqui, H., Mautner, A., Perez de Larraya, U., Pfenninger, N., Tingaut, P., and Zimmermann, T. (2016). "Cationic cellulose nanofibers from waste pulp residues and their nitrate, fluoride, sulphate and phosphate adsorption properties," *Carbohydrate Polymers* 135, 334-340. DOI: 10.1016/j.carbpol.2015.08.091
- Sirviö, J. A., Ismail, M. Y., Zhang, K., Tejesvi, M. V., and Ämmälä, A. (2020). "Transparent lignin-containing wood nanofiber films with UV-blocking, oxygen barrier, and anti-microbial properties," *Journal of Materials Chemistry A* 8(16), 7935-7946. DOI: 10.1039/C9TA13182E
- Trache, D., Donnot, A., Khimeche, K., Benelmir, R., and Brosse, N. (2014). "Physico-chemical properties and thermal stability of microcrystalline cellulose isolated from alfa fibres," *Carbohydrate Polymers* 104, 223-230. DOI: 10.1016/j.carbpol.2014.01.058
- Visakh, P. M., Thomas, S., Oksman, K., and Mathew, A. P. (2012). "Effect of cellulose nanofibers isolated from bamboo pulp residue on vulcanized natural rubber," *BioResources* 7(2), 2156-2168. DOI: 10.15376/biores.7.2.2156-2168
- Xiong, R., Zhang, X., Tian, D., Zhou, Z., and Lu, C. (2012). "Comparing microcrystalline with spherical nanocrystalline cellulose from waste cotton fabrics," *Cellulose* 19(4), 1189-1198. DOI: 10.1007/s10570-012-9730-4
- Yan, B., Zhang, S., Chen, W., and Cai, Q. (2018). "Pyrolysis of tobacco wastes for bio-oil with aroma compounds," *Journal of Analytical and Applied Pyrolysis* 136, 248-254. DOI: 10.1016/j.jaap.2018.09.016
- Yan, C. F., Yu, H. Y., and Yao, J. M. (2015). "One-step extraction and functionalization of cellulose nanospheres from lyocell fibers with cellulose II crystal structure," *Cellulose* 22(6), 3773-3788. DOI: 10.1007/s10570-015-0761-5
- Yang, H., Yan, R., Chen, H., Lee, D. H., and Zheng, C. (2007). "Characteristics of hemicellulose, cellulose and lignin pyrolysis," *Fuel* 86(12-13), 1781-1788. DOI: 10.1016/j.fuel.2006.12.013
- Yu, H. Y., Zhang, H., Song, M. L., Zhou, Y., Yao, J., and Ni, Q. Q. (2017). "From cellulose nanospheres, nanorods to nanofibers: Various aspect ratio induced nucleation/reinforcing effects on polylactic acid for robust-barrier food packaging," *ACS Applied Materials & Interfaces* 9(50), 43920-43938. DOI: 10.1021/acsami.7b09102
- Zhang, J., Elder, T. J., Pu, Y., and Ragauskas, A. J. (2007). "Facile synthesis of spherical cellulose nanoparticles," *Carbohydrate Polymers* 69(3), 607-611. DOI: 10.1016/j.carbpol.2007.01.019
- Zhang, S., Fu, C., Li, F., Yu, J., and Gu, L. (2009). "Direct preparation of a novel membrane from unsubstituted cellulose in NaOH complex solution," *Iranian Polymer Journal* 18(10), 767-776.

- Zhang, S., Li, F. X., Yu, J. Y., and Hsieh, Y. L. (2010). "Dissolution behaviour and solubility of cellulose in NaOH complex solution," *Carbohydrate Polymers* 81(3), 668-674. DOI: 10.1016/j.carbpol.2010.03.029
- Zhang, J., Zhang, J., Wang, M., Wu, S., Wang, H., Niazi, N. K., Man, Y. B., Christie, P., Shan, S., and Wong, M. H. (2019a). "Effect of tobacco stem-derived biochar on soil metal immobilization and the cultivation of tobacco plant," *Journal of Soils and Sediments* 19(5), 2313-2321. DOI: 10.1007/s11368-018-02226-x
- Zhang, S., Zhang, F., Jin, L., Liu, B., Mao, Y., Liu, Y., and Huang, J. (2019b). "Preparation of spherical nanocellulose from waste paper by aqueous NaOH/thiourea," *Cellulose* 26(8), 5177-5185. DOI: 10.1007/s10570-019-02434-9
- Zhang, S., Zhou, Y., Zhu, G., Jiang, Y., Xie, J., Qi, J., Yang, H., Hui, W., and Huang, J. (2021). "Enhancement of magnetic film with light penetration by immobilization of Fe₃O₄ nanoparticles in a spherical bamboo nanocellulose network," *Cellulose* 28(7), 4179-4189. DOI: 10.1007/s10570-021-03802-0
- Zhang, S., Xu, X., Ye, Z., Liu, Y., Wang, Q., Chen, Q., Jiang, Y., Qi, J., Tian, D., Xu, J., *et al.* (2023). "A large-nanosphere/small-nanosphere (cellulose/silver) antibacterial composite with prominent catalytic properties for the degradation of p-nitrophenol," *Applied Surface Science* 608, article ID 155192. DOI: 10.1016/j.apsusc.2022.155192

Article submitted: September 12, 2023; Peer review completed: October 14, 2023; Revised version received and accepted: April 25, 2024; Published: April 29, 2024.

DOI: 10.15376/biores.19.2.3826-3836